Title

Amino Acid-Derived Sensors for Specific Zn2+ Detection Using Hyperpolarized 13C Magnetic Resonance Spectroscopy

Journal

Chemistry - A European Journal, 25(51)

ISSN

0947-6539

Authors

Wang, Sinan
Korenchan, David E
Perez, Paola M
et al.

Publication Date

2019-09-12

DOI

10.1002/chem.201902771

Peer reviewed

Published in final edited form as:

Chemistry. 2019 September 12; 25(51): 11842–11846. doi:10.1002/chem.201902771.

Amino Acid-Derived Sensors For Specific Zn^{2+} Detection Using Hyperpolarized ^{13}C Magnetic Resonance Spectroscopy

Sinan Wang,
Department of Radiology and Biomedical Imaging, University of California, San Francisco, San Francisco, CA, USA 94107

David E. Korenchan,
Department of Radiology and Biomedical Imaging, University of California, San Francisco, San Francisco, CA, USA 94107

Paola M. Perez,
Department of Radiology and Biomedical Imaging, University of California, San Francisco, San Francisco, CA, USA 94107

Céline Taglang,
Department of Radiology and Biomedical Imaging, University of California, San Francisco, San Francisco, CA, USA 94107

Thomas R. Hayes,
Department of Radiology and Biomedical Imaging, University of California, San Francisco, San Francisco, CA, USA 94107

Renuka Sriram,
Department of Radiology and Biomedical Imaging, University of California, San Francisco, San Francisco, CA, USA 94107

Robert Bok,
Department of Radiology and Biomedical Imaging, University of California, San Francisco, San Francisco, CA, USA 94107

Andrew S. Hong,
Department of Radiology and Biomedical Imaging, University of California, San Francisco, San Francisco, CA, USA 94107

Yunkou Wu,
Department of Radiology, Johns Hopkins University, Baltimore, MD, USA 21287

Henry Li,
Department of Radiology and Biomedical Imaging, University of California, San Francisco, San Francisco, CA, USA 94107

Zhen Wang,
Department of Radiology and Biomedical Imaging, University of California, San Francisco, San Francisco, CA, USA 94107

robert.flavell@ucsf.edu.

John Kurhanewicz,
Department of Pharmaceutical Chemistry, University of California, San Francisco, San Francisco, CA, USA 94107

Department of Radiology and Biomedical Imaging, University of California, San Francisco, San Francisco, CA, USA 94107

David M. Wilson,
Department of Radiology and Biomedical Imaging, University of California, San Francisco, San Francisco, CA, USA 94107

Robert R. Flavell
Department of Pharmaceutical Chemistry, University of California, San Francisco, San Francisco, CA, USA 94107

Department of Radiology and Biomedical Imaging, University of California, San Francisco, San Francisco, CA, USA 94107

Abstract

Alterations in Zn^{2+} concentration are seen in normal tissues and in disease states, and for this reason imaging of Zn^{2+} is an area of active investigation. Herein, enriched [1-^{13}C]cysteine and [1-$^{13}C_2$]iminodiacetic acid were developed as Zn^{2+}-specific imaging probes using hyperpolarized ^{13}C magnetic resonance spectroscopy. [1-^{13}C]cysteine was used to accurately quantify Zn^{2+} in complex biological mixtures. These sensors can be employed to detect Zn^{2+} via imaging mechanisms including changes in ^{13}C chemical shift, resonance linewidth, or T_1.

Graphical abstract

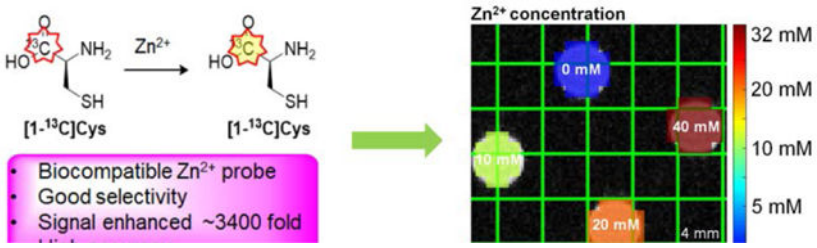

Enriched [1-^{13}C]cysteine and [1-$^{13}C_2$]iminodiacetic acid are developed as Zn^{2+}-specific imaging probes using hyperpolarized ^{13}C magnetic resonance spectroscopy. These sensors can be employed to detect Zn^{2+} via imaging mechanisms including changes in ^{13}C chemical shift, resonance linewidth, or T_1. [1-^{13}C]cysteine is able to accurately quantify Zn^{2+} in complex biological mixtures.

Keywords

imaging agents; zinc; hyperpolarization; ^{13}C MRI; chemical shift

Zinc (Zn^{2+}) is the second most abundant transition metal ion in the human body and plays various structural, regulatory and catalytic functions in physiology.[1,2] Multiple methods for

the measurement of Zn^{2+} concentration have been investigated as biomarkers for human disease, including blood and tissue tests, and imaging methods.[3] Existing imaging techniques include fluorescence and magnetic resonance-based approaches. Small-molecule fluorescent agents with varying Zn^{2+} affinities have been used to image live cells[4,5,6] Magnetic resonance imaging (MRI) using Zn^{2+}-responsive contrast agents has been proposed as an alternative imaging method that would allow non-invasive high-resolution monitoring of Zn^{2+} metabolism. Although there has been some success using manganese-derived probes[7] and paramagnetic chemical exchange saturation transfer agents,[8] most reported Zn^{2+}-responsive MRI agents are gadolinium-based.[9,10]

Enabled by hyperpolarization techniques such as dynamic nuclear polarization (DNP) and parahydrogen induced polarization (PHIP),[11–14] hyperpolarized (HP) probes for *in vivo* detection of a variety of analytes using HP ^{13}C MRS have been developed.[15,16] Hyperpolarized EDTA and EGTA were reported for multi-metal imaging.[17] Here, we explored the use of HP ^{13}C MRS for Zn^{2+}-specific imaging. In particular, we identified *L*-cysteine-1-^{13}C ([1-^{13}C]Cys) and iminodiacetic acid-1-$^{13}C_2$ ([1-$^{13}C_2$]IDA) as candidate probes that demonstrate altered magnetic properties upon binding Zn^{2+}, optimized their polarization parameters, and demonstrated that [1-^{13}C]Cys can accurately measure Zn^{2+} using ^{13}C HP MRS in phantoms and biological samples (Figure 1A).

We considered the requirements for a potential hyperpolarized Zn^{2+} imaging probe to include 1) a large change in ^{13}C chemical shift in the presence of Zn^{2+}, 2) good selectivity to Zn^{2+} over biologically abundant cations such as Ca^{2+} and Mg^{2+}, 3) insensitivity to changes in pH over the physiologic range, 4) a sufficient T_1 relaxation time for MRI, and 5) lack of known or predicted toxicity. We began our study by screening a variety of candidate Zn^{2+} ligands for their chemical shift response upon Zn^{2+} binding. Among the 34 tested compounds, 10 ligands demonstrated a chemical shift response to Zn^{2+} binding. We noted that ligands with logarithm of stability constants of Zn^{2+} (logK) greater than 6.9 all displayed a chemical shift response to Zn^{2+} binding, while ligands with logK lower than 5.2 did not have a chemical shift response to Zn^{2+} binding (SI Table S1). Ligands bearing a soft functional group such as pyridine tended to show a chemical shift response at lower Zn^{2+} stability constants while ligands with hard functional groups, such as hydroxyl showed a chemical shift response at higher stability constants. Cysteine and iminodiacetic acid were selected for further evaluation because of their large chemical shift response to Zn^{2+} binding (+4.6 and +7.3 ppm in the presence of equimolar Zn^{2+}, respectively), excellent water solubility, low molecular weight, predicting a long ^{13}C T_1, and convenience for ^{13}C labeling. ^{13}C-labeled cysteine was commercially available, and ^{13}C-labeled IDA was synthesized from [1-^{13}C]glycine and [1-^{13}C]methyl bromoacetate in 3 steps with a 32% total yield (Scheme 1). Their specificity for Zn^{2+} versus other abundant physiologic cations and their sensitivity to pH changes were also tested. Both probes showed excellent specificity for Zn^{2+} over other main physiologic cations Na^+, K^+, Ca^{2+} and Mg^{2+}, and limited chemical shift change over the physiologic pH range of 6.5 to 7.4 (Figure 1B). These preliminary investigations suggested that [1-^{13}C]Cys and [1-$^{13}C_2$]IDA would be specific and sensitive probes for detecting Zn^{2+} using HP ^{13}C MRI.

A quantitative method for determining Zn^{2+} concentration was developed for these probes using NMR. A titration curve was plotted to show the chemical shift difference between [1-^{13}C]Cys and internal standard urea as a function of the Zn^{2+} to [1-^{13}C]Cys ratio. The peak moved linearly with increasing Zn^{2+} up to 0.25 equivalents of Zn^{2+} to [1-^{13}C]Cys. The rate of chemical shift change decreased at higher Zn^{2+} concentrations (Figure 2A, 2B, SI Table S2, SI equation S1). This suggests that [1-^{13}C]Cys may have multiple Zn^{2+} binding conformations, as previously reported.[18,19] The manifestation of the ^{13}C signal as a single resonance indicates that the on-off rates for Zn^{2+} binding are rapid, compared with the absolute frequency difference between bound/unbound ^{13}C resonances. A linewidth change with different Zn^{2+}/[1-^{13}C]Cys ratios was also observed. In particular, the linewidth increased significantly at lower Zn^{2+} concentrations with the widest linewidth being between 0.2 eq and 0.5 eq of [1-^{13}C]Cys, thus demonstrating exchange broadening at different Zn^{2+}/[1-^{13}C]Cys ratios (SI Table S3). The chemical shift change of [1-^{13}C]Cys with equimolar Zn^{2+} was tested at different temperatures ranging from 20 °C to 50 °C and at various [1-^{13}C]Cys concentrations from 1 mM to 100 mM. These studies showed that the temperature and concentration of [1-^{13}C]Cys (in the presence of equimolar zinc) had little or no influence on the chemical shift response (SI Tables S3 and S4).

A similar titration method was utilized for IDA for quantitative determination of Zn^{2+} concentration. When Zn^{2+} was added to [1-$^{13}C_2$]IDA, a new resonance at a lower field appeared. The area under the peak (integration) increased linearly with increasing Zn^{2+} concentration from 0 to 0.5 equivalents of Zn^{2+} to [1-$^{13}C_2$]IDA, which indicates that [1-$^{13}C_2$]IDA binds to Zn^{2+} with a 2:1 probe:Zn stoichiometry, as previously reported (Figure 2C, 2D).[20] Additionally, the unbound [1-$^{13}C_2$]IDA peak demonstrated increasing line broadening in response to Zn^{2+} (SI Table S5). It is worth noting that the [1-$^{13}C_2$]IDA:Zn complex appears as two separate peaks while the [1-^{13}C]Cys:Zn complex appears as a single peak, indicating that the on and off rates for [1-$^{13}C_2$]IDA are slower than the frequency difference between bound and unbound resonances and the on and off rates for [1-^{13}C]Cys are more rapid. These results are analogous to prior findings in ^{15}N, ^{19}F, and hyperpolarized ^{13}C pH imaging probe development efforts.[21–27] Overall, these data demonstrate that the chemical shift of the 1-^{13}C NMR signal of cysteine and IDA change in a predictable and quantitative manner in response to Zn^{2+} concentration.

Next, we developed and optimized a hyperpolarization method for ^{13}C labeled [1-^{13}C]Cys and [1-$^{13}C_2$]IDA. For [1-^{13}C]Cys, the optimized preparation was obtained by a mixture of 1.0 eq of [1-^{13}C]Cys, 0.5 eq of 4N HCl and 2.65 eq of glycerol, with 20 mM OX063 radical.[28] Using this method, 13.4 ± 0.6% back-calculated polarization was obtained with a polarization time constant of 1227 ± 30 (n = 3). The T_1 relaxation time was 36.0 ± 1.8 seconds at a magnetic field of 3T. A Zn^{2+}-dependent decrease in T_1 of [1-^{13}C]Cys was observed when polarized [1-^{13}C]Cys was mixed with various equivalents of Zn^{2+}. A T_1 of 17.5 seconds was observed when 1 equivalent of Zn^{2+} was present (Table S6). For [1-$^{13}C_2$]IDA, the optimized preparation included a mixture of 1.0 eq of [1-$^{13}C_2$]IDA disodium salt, 14.0 eq of D_2O and 1.8 eq of DMSO, with 15 mM OX063.[17] Using this method, 6.6 ± 0.9% (n = 3) back-calculated polarization was obtained with the polarization time constant of 1480 ± 38 (n = 3). The T_1 was 39.3 ± 1.0 seconds at 3T. The T_1 of both bound and unbound [1-$^{13}C_2$]IDA resonances were also Zn^{2+} dependent, with the T_1

decreasing to 16.6 seconds when 1 eq of Zn^{2+} was present (Figure 3, SI Table S7). We hypothesize that the decrease in T_1 is due to an increase in molecular weight of the complex.[29] The high percent polarization, and relatively long T_1 of the Zn^{2+} ligands suggested feasibility for subsequent imaging experiments.

The ability of the probes to image Zn^{2+} concentration was tested using phantoms on a 3T MRI system. For cysteine, a copolarization method, as we have previously reported, was developed with [1-^{13}C]urea as a chemical shift standard.[23] A four-compartment phantom containing various Zn^{2+} concentrations in each compartment was prepared (Figure 4A, B). As in the thermal equilibrium measurements, a chemical shift change was observed in response to Zn^{2+} in the ^{13}C cysteine spectrum. By using the best-fit linear model of chemical shift asFigure 3 a function of Zn^{2+} concentration (Figure 2B inset), hyperpolarized [1-^{13}C]Cys was able to accurately determine the concentration over the physiologically relevant range of 0.2 – 20 mM Zn^{2+}. At the highest tested Zn^{2+} concentration of 40 mM, a slight deviation was observed, possibly due to signal loss and/or line broadening.

A phantom imaging experiment to determine the sensitivity showed that HP [1-^{13}C]Cys can detect 200 μM of Zn^{2+} when 4 mM of [1-^{13}C]Cys was present (Figure 4B). When hyperpolarized [1-$^{13}C_2$]IDA was tested in a phantom for Zn^{2+} imaging, the Zn^{2+} bound [1-$^{13}C_2$]IDA peak appeared when more Zn^{2+} was present. The line broadening of both the Zn^{2+} bound and unbound peaks of [1-$^{13}C_2$]IDA resulted in a loss of SNR between 0.2 eq Zn^{2+} and 0.3 eq Zn^{2+} (SI Figure S2). For this reason, accurate Zn^{2+} concentrations could not be obtained using this probe. Overall, these phantom experiments demonstrated that hyperpolarized [1-^{13}C]Cys is a sensitive and accurate Zn^{2+} biosensor over the physiologic range, while issues with line broadening and signal loss limit the applicability of [1-$^{13}C_2$]IDA.

Finally, we verified that HP [1-^{13}C]Cys could accurately determine Zn^{2+} concentration in biological samples (Figure 5) by comparing imaging results against a commercially available fluorescence based Zn^{2+} quantification kit. Rat serum and prostate extracts were selected as biological samples with low and high Zn^{2+} concentration, respectively. In these samples, the Zn^{2+} concentration was accurately measured at 0.1 and 1.9 mM, respectively. The HP and kit Zn^{2+} measurements agreed within 0.1 mM. In order to verify that the signal change in these samples represented a specific response to Zn^{2+}, additional tubes including serum spiked with exogenous Zn^{2+}, and a prostate sample with additional tris(2-pyridylmethyl)amine (TPA), a high-affinity and specific chelator, were investigated.[30] We found that the Zn^{2+} concentration was accurately measured in the spiked serum sample, and that the addition of the TPA to the prostate extract blocked the chemical shift change. These data confirm that Zn^{2+} is both necessary and sufficient to induce the chemical shift change in cysteine, and moreover that this probe accurately and specifically determines Zn^{2+} concentration in complex biological samples.

For future *in vivo* applications, [1-^{13}C]Cys in particular demonstrates both possible advantages and limitations compared against existing techniques. Owing to the short lifetime of the signal, it is unlikely that it would be internalized into cells in a time course reasonable to measure intracellular zinc concentration. Therefore, this method would likely be restricted

to extracellular space Zn^{2+} imaging. However, zinc can be secreted from tissues including pancreas and prostate in response to glucose treatment. For example, Sherry et al. have developed imaging methods to detect the release of Zn^{2+} ions from β-cells in response to high glucose,[31] as well as to differentiate between healthy and malignant prostate tissue in mouse models.[32] Such a model could applied for initial *in vivo* testing of these probes. An additional limitation could be metabolic transformation, which could confound interpretation of spectroscopic data. Toxicity concerns are unlikely based on the known toxicology profile of cysteine.[33] The majority of Zn^{2+} imaging probes are gadolinium-based contrast agents, which face the concern of their deposition in brain and environment, a concern which would be avoided in this case.[34] A final potential benefit of this method is the broad range of zinc concentration in serum and other tissues, potentially enabling high image contrast. Overall, these preliminary data suggest both possibilities and limitations for future *in vivo* applications of these methods.

Taken together, these data demonstrate that [1-^{13}C]Cys and [1-$^{13}C_2$]IDA represent promising probes for imaging Zn^{2+} using hyperpolarized ^{13}C MRI. The probes demonstrate large changes in signal and chemical shift in response to Zn^{2+}, excellent selectivity over other biologically relevant cations and changes in pH, favorable T_1 and polarization parameters, and can be imaged in phantom experiments. [1-^{13}C]Cys accurately quantified Zn^{2+} concentration in biological samples at physiologically relevant concentrations. For this reason, [1-^{13}C]Cys is a particularly promising probe for future *in vivo* hyperpolarized magnetic resonance imaging of pathologies with alterations in Zn^{2+} homeostasis such as prostate cancer, neurodegenerative disease, and diabetes.

Supplementary Material

Refer to Web version on PubMed Central for supplementary material.

Acknowledgements

R.R.F. acknowledges a Howard S. Stern award of the Society of Abdominal Radiology, a David Blitzer Prostate Cancer Foundation Young Investigator Award, a Department of Defense Prostate Cancer Research Program Physician Research Training Award, and NIH R21 EB026012–01.

References

[1]. Kambe T, Tsuji T, Hashimoto A, Itsumura N, Physiol. Rev. 2015, 95, 749–784. [PubMed: 26084690]

[2]. Vallee BL, Auld DS, Acc. Chem. Res. 1993, 26, 543–551.

[3]. Costello LC, Franklin RB, Mol. Cancer. 2006, 5, 1–13. [PubMed: 16403226]

[4]. Zhang XA, Hayes D, Smith SJ, Friedle S, Lippard SJ, J. Am. Chem. Soc. 2008, 130, 15788–15789. [PubMed: 18975868]

[5]. Komatsu K, Kikuchi K, Kojima H, Urano Y, Nagano T, J. Am. Chem. Soc. 2005, 127, 10197–10204. [PubMed: 16028930]

[6]. Tsien RY, Nat. Cell Biol. 2003, 16–21. [PubMed: 12511887]

[7]. Zhang X, Lovejoy KS, Jasanoff A, Lippard SJ, Proc. Natl. Acad. Sci. 2007, 104, 10780–10785. [PubMed: 17578918]

[8]. Trokowski R, Ren J, Kálmán FK, Sherry AD, Angew. Chemie. Int. Ed. 2005, 44, 6920–6923.

[9]. Lo ST, Martins AF, Jordan VC, Sherry AD, Isr. J. Chem. 2017, 57, 854–886. [PubMed: 30319140]

[10]. Esqueda AC, López JA, Andreu-de-Riquer G, Alvarado-Monzón JC, Ratnakar J, Lubag AJM, Sherry AD, De León-Rodríguez LM, J. Am. Chem. Soc. 2009, 131, 11387–11391. [PubMed: 19630391]

[11]. Gram A, Hansson G, Hansson L, Lerche MH, Ardenkjær-larsen JH, Servin R, Thaning M, Golman K, 2003, 100, 10158–10163.

[12]. Golman K, Axelsson O, Jo H, Månsson S, Olofsson C, Petersson JS, Magn. Reson. Med. 2001, 5, 1–5.

[13]. Leunbach I, Mansson S, Petersson JS, Ardenkjaer-Larsen JH, Golman K, Proc. Natl. Acad. Sci. 2003, 100, 10435–10439. [PubMed: 12930896]

[14]. Nikolaou P, Goodson BM, Chekmenev EY, Chem. -A Eur. J. 2015, 21, 3156–3166.

[15]. Day SE, Kettunen MI, Gallagher FA, Hu DE, Lerche M, Wolber J, Golman K, Ardenkjaer-Larsen JH, Brindle KM, Nat. Med. 2007, 13, 1382–1387. [PubMed: 17965722]

[16]. Bhattacharya P, Chekmenev EY, Reynolds WF, Wagner S, Zacharias N, Chan HR, Bünger R, Ross BD, NMR Biomed. 2011, 24, 1023–1028. [PubMed: 21538638]

[17]. Mishra A, Pariani G, Oerther T, Schwaiger M, Westmeyer GG, Anal. Chem. 2016, 88, 10790–10794. [PubMed: 27766840]

[18]. Shindo H, Brown TL, J. Am. Chem. Soc. 1965, 87, 1904–1909. [PubMed: 14290272]

[19]. Li NC, Manning RA, J. Am. Chem. Soc. 1955, 77, 5225–5228.

[20]. Ni LB, Zhang RH, Liu QX, Xia WS, Wang H, Zhou ZH, J. Solid State Chem. 2009, 182, 2698–2706. [PubMed: 20161370]

[21]. Düwel S, Hundshammer C, Gersch M, Feuerecker B, Steiger K, Buck A, Walch A, Haase A, Glaser SJ, Schwaiger M, Schilling F, Nat. Commun. 2017, 1–9. [PubMed: 28232747]

[22]. Korenchan DE, Taglang C, Von Morze C, Blecha JE, Gordon JW, Sriram R, Larson PEZ, Vigneron DB, Vanbrocklin HF, Kurhanewicz J, Wilson DM, Flavell RR, Analyst 2017, 142, 1429–1433. [PubMed: 28322385]

[23]. Flavell RR, Von Morze C, Blecha JE, Korenchan DE, Van Criekinge M, Sriram R, Gordon JW, Chen H, Subramaniam S, Bok RA, Wang Z, Vigneron D, Larson P; Kurhanewicz J, Wilson DM, Chem. Commun. 2015, 51, 14119–14122.

[24]. Gallagher FA, Kettunen MI, Day SE, Hu DE, Ardenkjær-Larsen JH, Zandt RI, Jensen PR, Karlsson M, Golman K, Lerche MH, Brindle KM, Nature 2008, 453, 940–943. [PubMed: 18509335]

[25]. Jiang W, Lumata L, Chen W, Zhang S, Kovacs Z, Sherry AD, Khemtong C, Sci. Rep. 2015, 5, 9104. [PubMed: 25774436]

[26]. Shchepin RV, Barskiy DA, Coffey AM, Theis T, Shi F, Warren WS, Goodson BM, Chekmenev EY, ACS Sensors 2016, 1, 640–644. [PubMed: 27379344]

[27]. Shchepin RV, Goodson BM, Theis T, Warren WS, Chekmenev EY, ChemPhysChem 2017, 18, 1961–1965. [PubMed: 28557156]

[28]. Jensen PR, Karlsson M, Meier S, Duus J, Lerche MH, Chem. -A Eur. J. 2009, 15, 10010–10012.

[29]. Keshari KR, Wilson DM, Chem. Soc. Rev. 2014, 43, 1627–1659. [PubMed: 24363044]

[30]. Huang Z, Zhang X, Bosch M, Smith SJ, Lippard SJ, Metallomics 2013, 5, 648–655. [PubMed: 23715510]

[31]. Lubag AJM, De Leon-Rodriguez LM, Burgess SC, Sherry AD, Proc. Natl. Acad. Sci. 2011, 108, 18400–18405. [PubMed: 22025712]

[32]. Preihs C, Zhang S, Lo ST, Chen S, Li WH, Clavijo Jordan MV, Lubag AJM, De Leon-Rodriguez LM, Rofsky NM, Sherry AD, Proc. Natl. Acad. Sci. 2016, 113, 5464–5471.

[33]. Lewis RJ Sr (ed), Sax's Dangerous Properties of Industrial Materials, 11th Edition Wiley-Interscience, Wiley & Sons, Inc Hoboken, NJ 2004, p1059.

[34]. Guo BJ, Yang ZL, Zhang LJ, Front. Mol. Neurosci. 2018, 11, 1–12. [PubMed: 29403353]

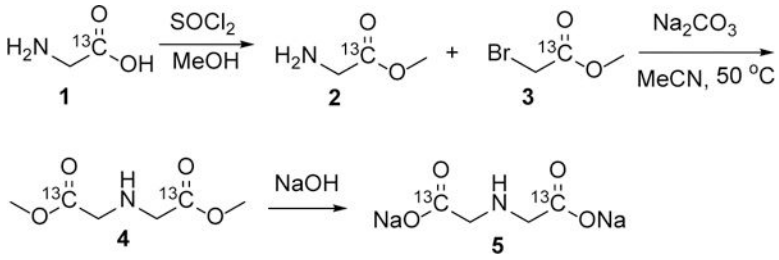

Scheme 1.
Synthesis of [1-$^{13}C_2$]IDA disodium salt.

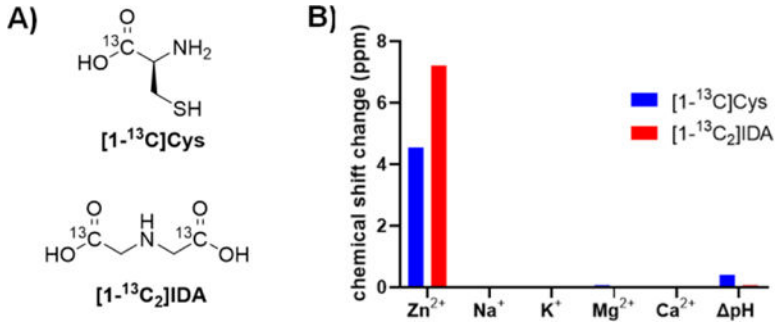

Figure 1.

Approach to specific detection of Zn^{2+} via hyperpolarized magnetic resonance spectroscopy (A) Structures of [1-^{13}C]Cys and [1-$^{13}C_2$]IDA. (B) Specificity of 50 mM [1-^{13}C]Cys and [1-$^{13}C_2$]IDA for physiological cations (present at 1 equivalent). pH-dependence of chemical shift was measured at pH 7.4 and 6.5, the physiologically relevant extracellular range.

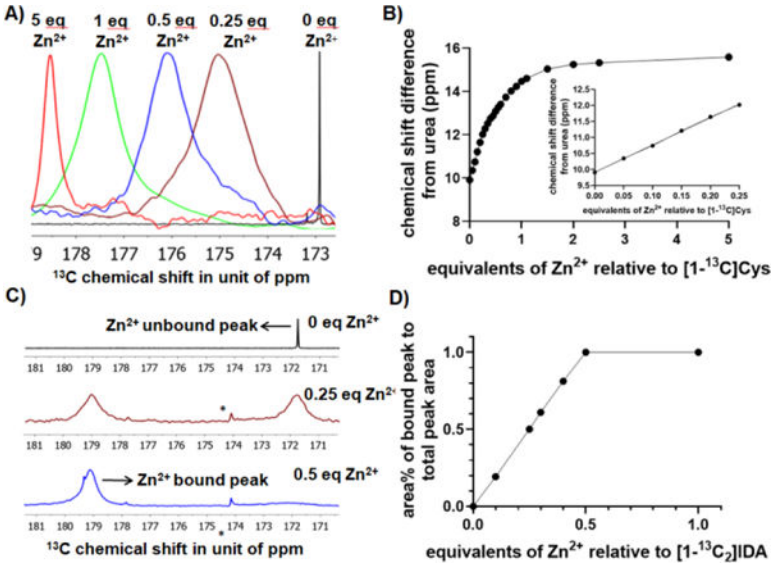

Figure 2.

Response of [1-^{13}C]Cys and [1-$^{13}C_2$]IDA to Zn^{2+} can be detected by several magnetic resonance mechanisms. (A) ^{13}C NMR Spectra for 50 mM [1-^{13}C]Cys with varying Zn^{2+} concentrations (B) Standard titration curve of [1-^{13}C]Cys in response to various Zn^{2+} concentrations. The insert shows the titration curve at low Zn^{2+} equivalents. (C) Spectra for 50 mM [1-$^{13}C_2$]IDA with various Zn^{2+} concentrations highlighting formation of a Zn^{2+} bound species, and increased linewidth upon Zn^{2+} binding. * represents natural abundance citric acid peak (D) Standard titration curve of [1-$^{13}C_2$]IDA.

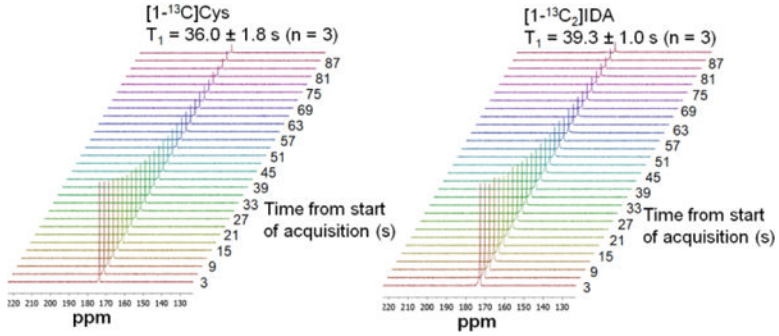

Figure 3.

Dynamic ^{13}C NMR spectra following polarization of [1-^{13}C]Cys (left) and [1-$^{13}C_2$]IDA (right). Pulse conditions were TR = 3s, 5º hard pulses, 10 kHz spectral width, 30 timepoints, nominal spectral resolution = 0.5 Hz.

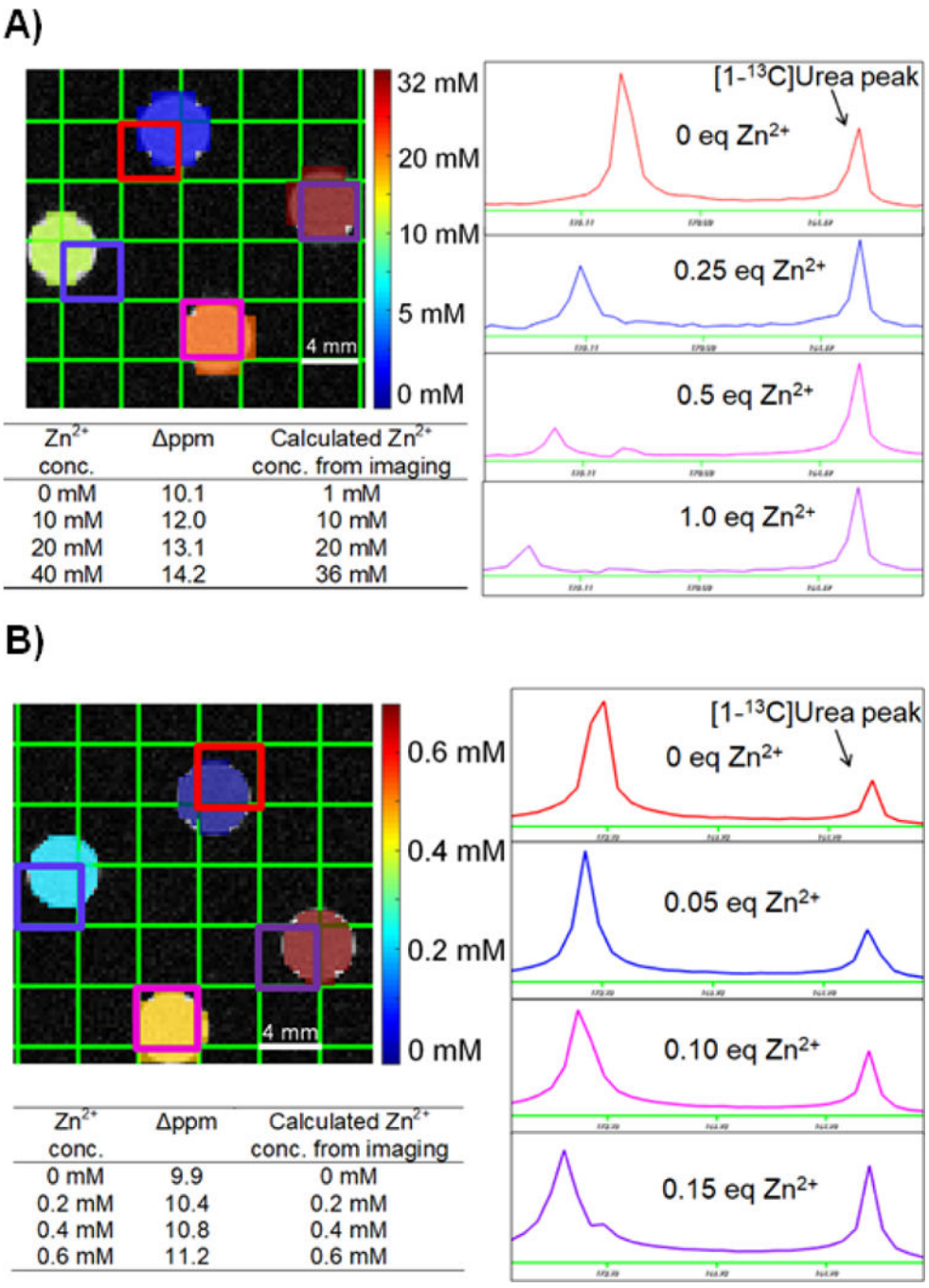

Zn^{2+} conc.	Δppm	Calculated Zn^{2+} conc. from imaging
0 mM	10.1	1 mM
10 mM	12.0	10 mM
20 mM	13.1	20 mM
40 mM	14.2	36 mM

Zn^{2+} conc.	Δppm	Calculated Zn^{2+} conc. from imaging
0 mM	9.9	0 mM
0.2 mM	10.4	0.2 mM
0.4 mM	10.8	0.4 mM
0.6 mM	11.2	0.6 mM

Figure 4.

HP [1-^{13}C]Cys accurately quantifies Zn^{2+} concentration in phantom imaging experiments through use of chemical shift measurements. (A) Phantom imaging conducted using 40 mM [1-^{13}C]Cys. (B) Phantom experiment conducted using 4 mM [1-^{13}C]Cys, indicating high sensitivity for low concentrations of Zn^{2+}.

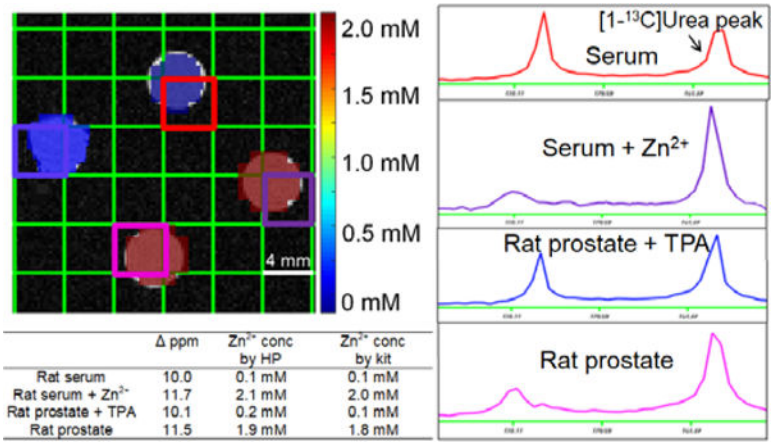

	Δ ppm	Zn^{2+} conc by HP	Zn^{2+} conc by kit
Rat serum	10.0	0.1 mM	0.1 mM
Rat serum + Zn^{2+}	11.7	2.1 mM	2.0 mM
Rat prostate + TPA	10.1	0.2 mM	0.1 mM
Rat prostate	11.5	1.9 mM	1.8 mM

Figure 5.

Hyperpolarized [1-^{13}C]Cys phantom imaging experiment demonstrating accurate Zn^{2+} quantification in biological samples. Accurate detection of Zn^{2+} concentration in presence of exogenous Zn^{2+} and in the presence of Zn^{2+}-chelating TPA demonstrates specificity of the probe for Zn^{2+} over other endogenous analytes.